JOURNAL OF MATERIALS SCIENCE 29 (1994) 3433–3440

Novel alkali-resistant porous glass prepared from a mother glass based on the SiO_2–B_2O_3–RO–ZrO_2 (R = Mg, Ca, Sr, Ba and Zn) system

T. YAZAWA, H. TANAKA
Osaka National Research Institute, Midorigaoka, Ikeda city, Osaka, 563 Japan
K. EGUCHI
Seiwadai-nishi, Kawanishi City, Hyogo, 666-01 Japan
S. YOKOYAMA
Akagawa Koshitu Glass Kogyosho Co., Ikue, Asahi-ku, Osaka, 535 Japan

The alkali-resistant porous glass was prepared from the SiO_2–B_2O_3–RO (R = Mg, Ca, Sr, Ba and Zn) system containing ZrO_2. The porous glass skeleton contained 2–3 mass % ZrO_2 and the alkali resistance was greatly improved over that of ordinary Vycor-type porous glass. Because of the high alkali resistance, the elimination of the colloidal SiO_2 and ZrO_2 gelated during the acid leaching of the phase-separated glass, was promoted and as a result, a very sharp pore-size distribution of porous glass was attained. In addition, the limit of the available pore size of porous glass was widely expanded.

1. Introduction

The ordinary Vycor-type porous glass has been extensively used as membranes for ultrafiltration and liquid and gas separation, packing materials in chromatography, adsorbents, and a carrier for catalysts and enzymes, though this type of porous glass has some defects. The water and alkali resistance is insufficient and the practically available pore diameter is restricted from 4–150 nm. In practice, it is important to obtain porous glasses with high alkali and water resistance for the following reasons. In the acid-leaching process of phase-separated glasses to obtain porous glasses, colloidal SiO_2 is deposited in the pores originating in the phase-separated structure [1]. This colloidal SiO_2 is caused by the gelation of the SiO_2 component distributed in the acid-soluble borate-rich phase of the phase-separated glass during the acid treatment. In order to avoid the gelation of SiO_2, a very large quantity of acid solution is required. For instance, in a pipe-shaped sample 0.5 mm thick, the quantity of acid solution used to leach 1 g phase-separated glass (bath ratio), must be more than 1 dm^3 [2]. Once the gelated SiO_2 forms, elimination is difficult because powerful washing spoils the porous glass itself. If a porous glass has a sufficient chemical resistance, gelated SiO_2 deposited in the pores can be easily eliminated without damage to the porous glass skeleton. Subsequently, a porous glass which has a sharp pore-size distribution can be obtained economically. Moreover, because amorphous SiO_2 has a water solubility of about 100 p.p.m. at room temperature [3], it is difficult to apply the ordinary Vycor-type porous glass in aqueous solution for a long time. This is a major barrier when porous glass is used as a membrane.

Research and development of glass fibre-reinforced cement has clarified that alkali resistance of glass can be markedly improved by the addition of ZrO_2 to the glass composition [4]. The present authors have reported that ZrO_2 can be introduced into the siliceous skeleton of the porous glass using SiO_2–B_2O_3–RO–ZrO_2 (R = Mg, Ca, Sr, Ba and Zn) glass as the mother glass [5, 6]. This system has not been studied as comprehensively as the mother glass of porous glass. Only a few reports have been published about this glass system by Voldan [7] and Taylor and Owen [8] in the research on potential host matrices for the incorporation of highly radioactive waste from nuclear reactors.

In this paper, a novel alkali-resistant porous glass prepared from mother glass based on this system, is described in detail.

2. Experimental procedure

2.1. Preparation of the mother glass

The glass formation region and the stability against opacification during cooling were observed for the SiO_2–B_2O_3–RO–ZrO_2 systems. The glasses were prepared by mixing the desired amount of optical-grade SiO_2 and reagent-grade $Al(OH)_3$, H_3BO_3, Na_2CO_3, ZrO_2 and RO or RCO_3. The powdered mixture was melted at 1400 °C for 3 h in alumina crucibles in an electric furnace, and then cast on a steel plate. Each

0022–2461

TABLE I Composition of the mother glass of porous glass

Mother glass	Composition (mol %)						Radius of R^{2+} (nm)
	SiO_2	B_2O_3	Na_2O	RO	ZrO_2	Al_2O_3	
G–O	66.4	22.8	5.7	–	3.2	1.9	
G–1	57.2	22.8	5.7	R = Mg 9.2	3.2	1.9	0.066
P–Ca	57.2	22.8	5.7	Ca 9.2	3.2	1.9	0.099
G–2	57.2	22.8	5.7	Sr 9.2	3.2	1.9	0.116
G–3	57.2	22.8	5.7	Ba 9.2	3.2	1.9	0.136
G–4	57.2	22.8	5.7	Zn 9.2	3.2	1.9	0.071

time 250 g glass was melted. Two glass compositions, listed in Table I as P–Ca and P–Zn, were adopted as the mother glasses to study the characteristics of the porous glasses.

2.2. Phase-separation treatment, acid and alkali leaching

The phase separation was carried out at 600–800 °C for 1–100 h. The borate-rich phase was leached with an aqueous solution of 1N HNO_3 for 48 h at 98 °C. The amount of acid used to leach out 1 g phase-separated glass (bath ratio) was 10 $cm^3 g^{-1}$. This corresponds to less than 1/100 of that necessary to obtain ordinary Vycor-type porous glass without gelated SiO_2. The use of H_2SO_4 was avoided in the first acid treatment to prevent the sedimentation of alkaline-earth metal sulphates. In the case of mother glasses which do not contain calcium, strontium or barium, this caution is not necessary. Thereafter, samples were leached again in an aqueous solution of 3N H_2SO_4 at 98 °C for 48 h to dissolve colloidal ZrO_2, which was produced from the ZrO_2 component of the soluble borate-rich phase and gelated during the first acid treatment similarly to the gelated SiO_2. The bath ratio of the second acid treatment was the same as the first HNO_3 treatment. Then glass samples were immersed in a solution of 0.4 N NaOH at 30 °C for 5 h to remove gelated SiO_2. The bath ratio in alkali treatment was 20 $cm^3 g^{-1}$. Finally, the samples were washed with water and dried to obtain porous glass samples.

2.3. Measurement of pore characteristics

Pore-size distribution of the porous glasses was measured by the mercury penetrating method (Porosimeter Model 200, Carlo Erba Co., Ltd) for pore diameters larger than 10 nm. The pores with diameter less than 10 nm were estimated from the nitrogen adsorption isotherms using the Cranston–Inkley method [9] with a Sorptmatic 1800 (Carlo Erba Co., Ltd). Prior to the measurement, the samples were heated at 150 °C for 2 h under a reduced pressure of 452 Pa.

2.4. Analysis of porous glass constituents

The porous glass samples were melted with sodium carbonate in a platinum crucible and analysed for SiO_2 and B_2O_3 by the perchloric acid dehydration and mannitol methods, respectively [10]. The other constituents were analysed using an induction-coupled plasma (ICP) analyser model SPS 1200A (Seiko Co.) after dissolution in a solution of 46.5 % and HF 35% HCl (HF : HCl = 1 : 2 in volume ratio). The leaching solutions were also analysed to evaluate the composition of the soluble phase.

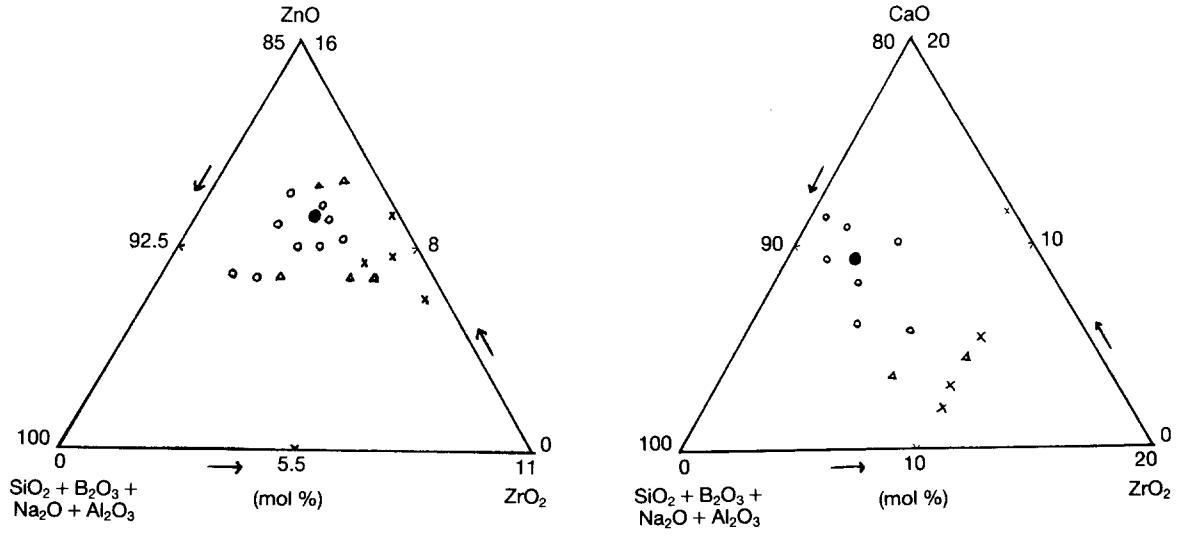

Figure 1 Glass-forming region of the mother glasses: (○) clear glass, (△) immiscible opaque glass, (×) incomplete melting, and (●) composition adopted in this work.

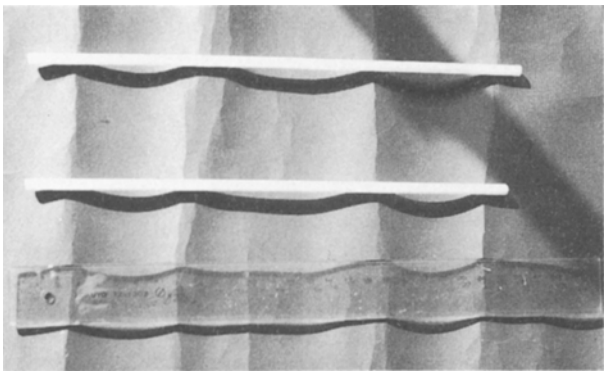

Figure 2 Porous glass samples prepared from P–Ca glass. The length of the scale is 30 cm.

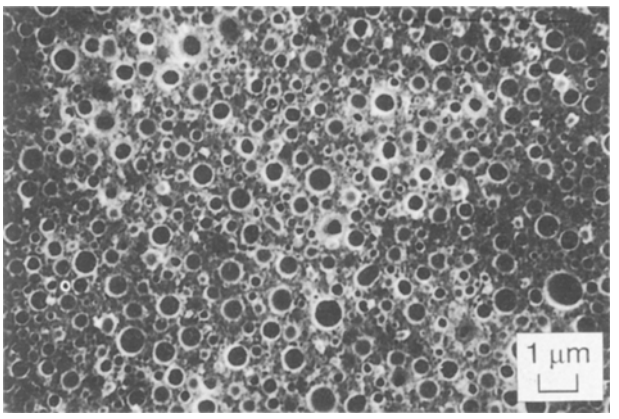

Figure 3 Scanning electron micrograph of the G-1 glass phase separated at 750 °C for 10 h.

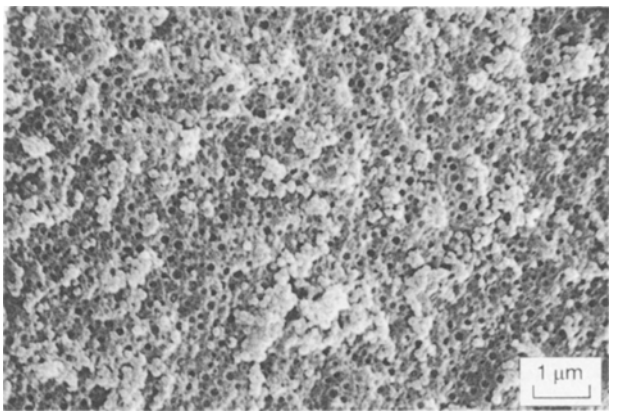

Figure 4 Scanning electron micrograph of the G-4 glass phase separated at 750 °C for 10 h.

2.5. Measurement of alkali resistance

The porous glass samples were dipped in 1N NaOH aqueous solution at 80 °C for the prescribed time. After neutralization with 1N HNO_3 and rinsing, the sample was dried sufficiently at 130 °C for 2 h in the evacuated condition and then weighed. The alkali resistance of the porous glass was determined from the weight loss ratio. All the porous glass samples tested had almost the same surface area, $\sim 8\ m^2\ g^{-1}$.

2.6. SEM observation

Porous glasses and phase-separated glasses were observed using an SEM model JSM-T100 (Nihon Electron K. K.) after gold-coating. Figs 1 and 2 were taken after etching the phase-separated glasses with 3% HF aqueous solution for 30 s.

3. Results

3.1. Glass-forming region

The melt of the SiO_2–B_2O_3–RO–ZrO_2 system shows a strong tendency to opacify during the cooling process. However, the glass formation of this system is facilitated by adding Na_2O and Al_2O_3. Fig. 1 shows the glass-forming region of the mother glass in the case of R = Ca and Zn. Among the glasses shown in Fig. 3, the glass with composition $57.2SiO_2 \cdot 22.8B_2O_3 \cdot 5.7Na_2O \cdot 9.2CaO \cdot 3.2ZrO_2 \cdot 1.9Al_2O_3$ (mol %, P–Ca glass) and $67.5SiO_2 \cdot 14.9B_2O_3 \cdot 5.1Na_2O \cdot 9.2ZnO \cdot 2.7ZrO_2 \cdot 0.6Al_2O_3$ (mol %, P–Zn glass) were confirmed to be the best, because they were stable against the opacification during cooling and easily shaped. The glass samples were not damaged during the acid and alkali treatment and therefore shaped porous glass samples such as sheets, tubes, capillaries and rods were easily prepared [11] as indicated in Fig. 4. Therefore, they were adopted as the mother glasses to study the characteristics of the porous glasses.

3.2. Tendency towards phase separation

3.2.1. Effect of RO constituent

Table I shows the mother glass composition tested to clarify the effect of RO component where the addition of RO is fixed at 9.2 mol %. These glasses were heat treated at 750 °C for 10 h and then treated with 1N HNO_3 at 98 °C for 48 h. Table II shows the pore characteristics of the porous glasses obtained from these mother glasses. Figs 1 and 2 show scanning electron micrographs of the phase-separation structure of G-1 and G-4 glasses, respectively. G-1 glass containing MgO and G-4 glass containing ZnO show droplet structure and cannot be leached by the acid. G-1 glass, however, gives porous glass samples of 73 nm pore diameter when phase separated at 700 °C for 10 h. On the other hand, no phase separation was observed in G-3 glass containing BaO heat treated at 750 °C and even at 800 °C. This fact suggests that G-3 has a low miscibility temperature or no tendency towards phase separation.

TABLE II Pore characteristics of the porous glass

Porous glass	Median diameter (nm)	Pore volume ($cm^3\ g^{-1}$)
G–0	Collapse during alkali treatment	
G–1	Droplet decomposition	(see Fig. 4)
P–Ca	405	0.32
G–2	217	0.85
G–3	No phase separation	
G–4	Droplet decomposition	(see Fig. 5)

3.2.2. Effect of CaO addition

Fig. 5 shows the median pore diameter of porous glasses obtained from the mother glasses with composition $(59.5 - x)SiO_2 \cdot 22.8B_2O_3 \cdot 5.7Na_2O \cdot (6.9 + x)CaO \cdot 3.2ZrO_2 \cdot 1.9Al_2O_3$ (x = 0–2.3) after heat treatment at 750 °C for 10 h. It is clear that CaO is effective in promoting phase separation because the pore diameter of porous glass considerably increases with increasing amount of CaO added in the mother glass.

3.3. Effect of heat-treatment conditions on phase separation

Fig. 6 shows the relation between median pore diameter and heat-treatment conditions for phase separation of P–Ca. Fig. 7 shows the pore-size distribution curves of porous glasses prepared from P–Zn. The pore diameter of the porous glasses increases with increase in the temperature and time of phase separation. This is in agreement with the ordinary Vycor-type porous glass. The pore size of P–Zn derived porous glasses is smaller than that of P–Ca derived porous glasses at the same heat-treatment conditions. The pore diameter obtained by this process ranges some tens of nanometres to about 10 μm, as shown in Figs 6 and 7. The limit of the available pore size of porous glass is thus widely expanded in comparison with 4–150 nm of the ordinary Vycor-type porous glass.

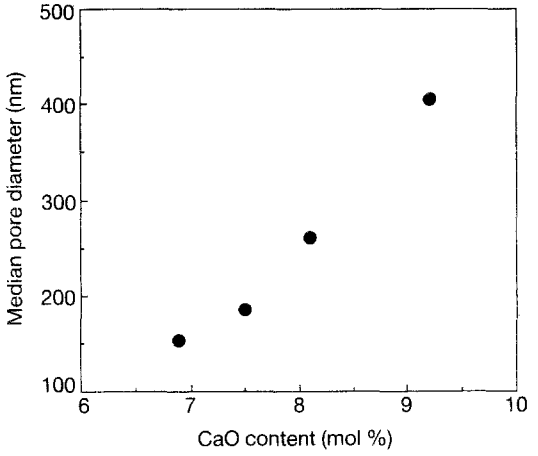

Figure 5 Relation between CaO content of mother glass and median pore diameter of porous glass. Glass composition: $(59.3 - x)SiO_2 \cdot 22.8B_2O_3 \cdot 5.7Na_2O \cdot (6.9 + x)CaO \cdot 3.2ZrO_2 \cdot 1.9Al_2O_3$, x = 0–2.3. Phase separation conditions: 750 °C, 10 h.

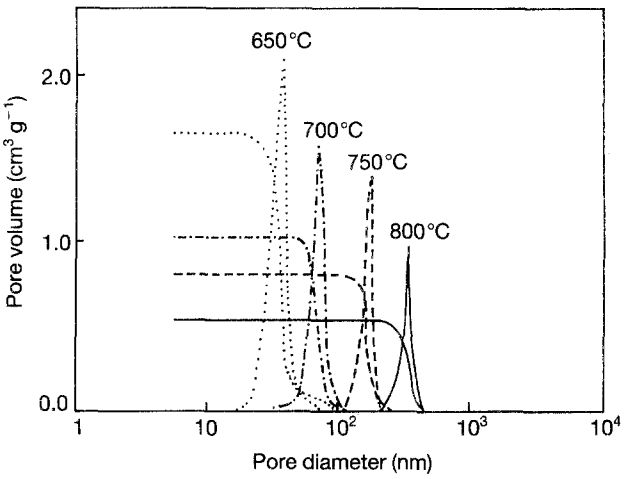

Figure 7 Pore-size distribution of porous glass prepared from P–Zn glass. Heat treatment time: 10 h.

3.4. Composition of porous glass

3.4.1. Variation of composition of porous glass with acid and alkali treatment

Fig. 8 shows the variation of composition of P–Ca glass with acid and alkali treatment. The SiO_2 content increases with the dissolution of soluble borate phase during the first HNO_3 treatment and simultaneously the B_2O_3 content decreases. The ZrO_2 content decreases after H_2SO_4 treatment due to the dissolution of colloidal ZrO_2 gelated during the first HNO_3 treatment. The increase in pore size accompanied by the

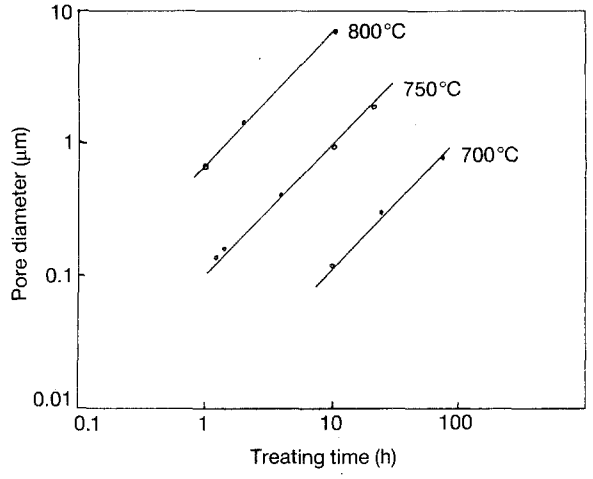

Figure 6 Relation between temperature and time of phase separation and median pore diameter of porous glass prepared from P–Ca glass.

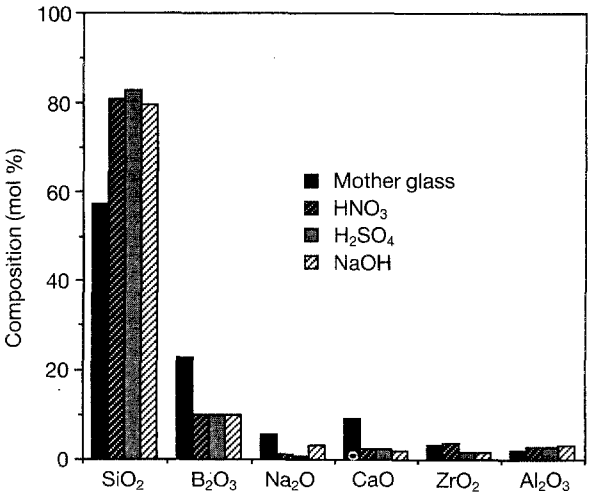

Figure 8 Variation of composition of P–Ca-derived porous glass with acid and alkali treatment.

dissolution of gelated ZrO_2 is shown in Fig. 9, where the decrease in specific surface area and increase in pore volume are also noted. After the final alkali treatment, the ZrO_2 content of 2–3 mass % is obtained. Fig. 10 shows a scanning electron micrograph of the porous glass after the final alkali treatment. The pore structure originated in the phase separation is clearly observed, verifying that the gelated materials are completely eliminated.

The porous glass finally obtained contains a much higher concentration of B_2O_3 and Al_2O_3 than the ordinary Vycor-type porous glasses and still contains the other components in considerable concentrations. Accordingly, the SiO_2 content is as low as 70–80 mol %.

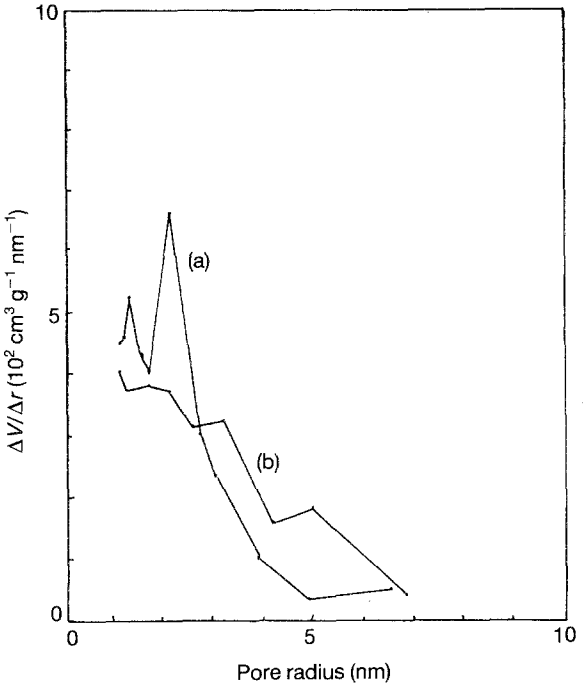

Figure 9 Pore-size distribution of P–Ca-derived porous glass after (a) HNO_3 and (b) H_2SO_4 treatment. Heat treatment: 750 °C, 10 h. (a) Surface area = 101 m^2 g^{-1}, pore volume = 0.12 cm^3 g^{-1}; (b) surface area = 77 m^2 g^{-1}, pore volume = 0.14 cm^3 g^{-1}.

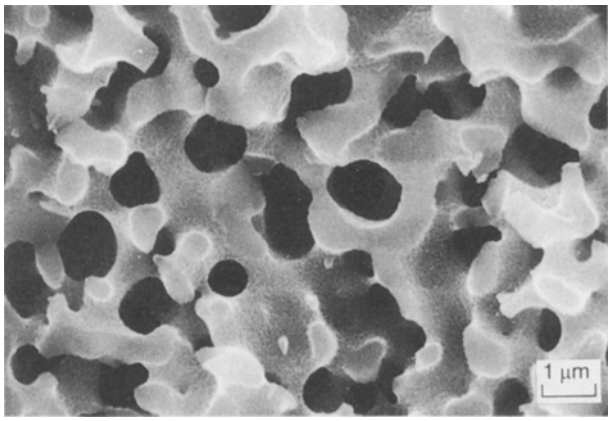

Figure 10 Scanning electron micrograph of the porous glass prepared from P–Ca glass. Heat treatment: 750 °C, 10 h.

3.4.2. Composition dependence of porous glass on phase-separation temperature

Fig. 11 shows the composition of the SiO_2-rich and B_2O_3-rich phases in phase-separated P–Ca glass. The composition of the B_2O_3-rich phase was determined by chemical analysis of the leaching solution. Most of the CaO is transferred to the B_2O_3-rich phase and ZrO_2 and Na_2O are also appreciably distributed in that phase. Al_2O_3 is distributed in the SiO_2-rich phase considerably, and in this phase the mole ratio Na_2O/Al_2O_3 approximately equals 1. This fact is confirmed by the results shown in Table III, where the composition of porous glasses prepared from P–Ca glass with varied heat-treatment temperature is compared. As shown in Table III, the CaO content is almost constant at different phase-separation temperatures, though the ZrO_2 and Al_2O_3 contents increase with increase in heat-treatment temperature. Fig. 12 shows ZrO_2 content of the porous glasses prepared by phase separation at 650–800 °C for 5 h (P–Ca glass) and 10 h (P–Zn glass). The increase in the ZrO_2 content of the porous glasses with increasing heat-treatment temperature is clearly shown. This is ascribed to the mutual approach of the composition of the silica-rich and borate-rich phases with increase in temperature, because the major part of ZrO_2 is distributed in the soluble borate-rich phase, as shown in Fig. 11.

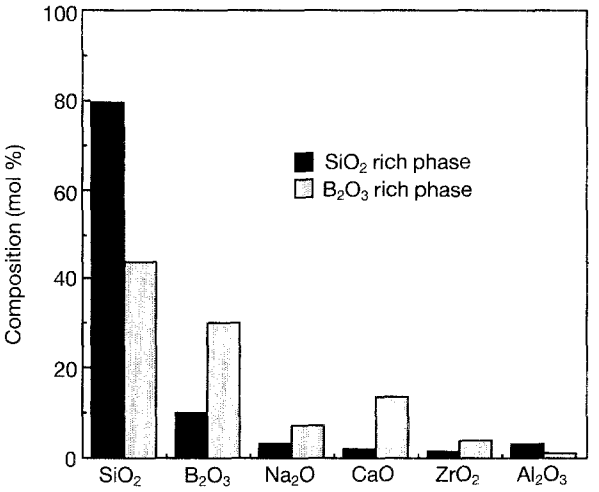

Figure 11 Composition of SiO_2-rich and B_2O_3-rich phase of P–Ca glass heat treated at 760 °C, 5 h.

TABLE III Composition of porous glass prepared from P–Ca glass after heat treatment at various temperatures for 5 h

Heat-treatment temperature (°C)	Composition (mol %)					
	SiO_2	B_2O_3	Na_2O	CaO	ZrO_2	Al_2O_3
730	73.7	18.6	2.1	1.96	1.18	2.45
740	73.1	19.5	2.2	1.86	1.27	2.15
750	75.5	16.6	2.6	1.95	1.27	2.14
760	79.4	10.2	3.1	1.94	1.55	3.10

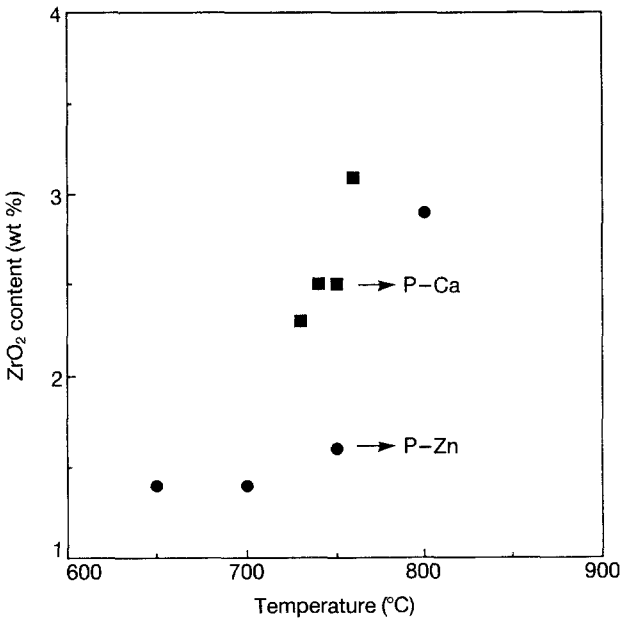

Figure 12 Dependence of ZrO_2 content of porous glass, prepared from P–Ca and P–Zn, on the phase-separation temperature. Heat treatment time: 5 h (P–Ca), 10 h (P–Zn).

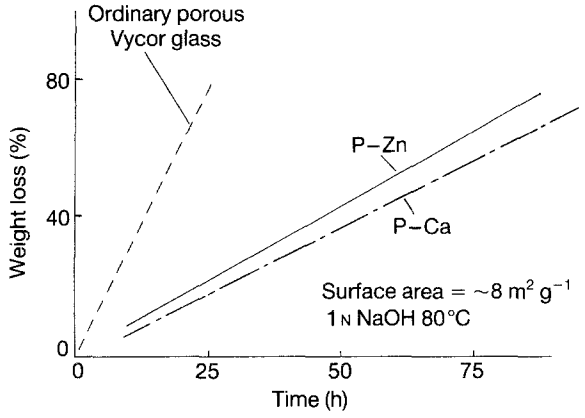

Figure 13 Alkali resistance of ordinary Vycor-type porous glass and P–Ca and P–Zn derived porous glasses.

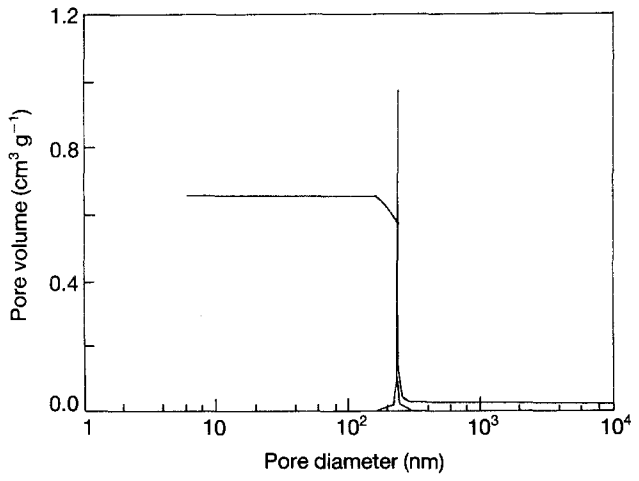

Figure 14 The occurrence of a very narrow pore-size distribution obtained in P–Zn derived porous glass. Phase separation conditions: 800 °C, 6 h.

3.5. Alkali resistance

Fig. 13 shows the results of the alkali resistance test of porous glasses prepared from mother glasses P–Ca and P–Zn. The alkali resistance of these porous glasses is by far greater than that of the ordinary Vycor-type porous glass. Moreover the pore size distribution of the porous glasses meticulously prepared from these mother glasses is very sharp as shown in Fig. 14. This is ascribed to the fact that the porous glass is free from the gelated SiO_2 or ZrO_2, at least in part.

4. Discussion

4.1. Tendency towards phase separation

In the SiO_2–RO glass systems, the phase separation is caused by the competition for oxygen anions between metal ions and Si^{4+} ions. Accordingly, the larger the cationic field of the metal ions, the larger is the tendency towards phase separation [12]. Here, the cationic field is expressed as $F = z/r$ (z is the cationic charge, namely 2 for alkaline-earth metal and zinc, r is the cation radius).

The RO component introduced into the SiO_2–B_2O_3 system alters the boron–oxygen coordination structure from a $[BO_3]$ triangle to a $[BO_4]$ tetrahedron. The four oxygen ions forming the $[BO_4]$ tetrahedron are substantially bridging in the composition range of this work, and accordingly each $[BO_4]$ tetrahedron carries an electric charge of -1. One R^{2+} ion compensates the charge of two $[BO_4]$ tetrahedra, causing strain in the boron–oxygen network. As a result, the compatibility of the boron–oxygen network with the silicon–oxygen network decreases remarkably. Thus the tendency towards phase separation is expected to increase with increasing cationic field of the R^{2+} ions also in this system.

In view of Table II and the facts described in Section 3.2.1, the order of the effect of the RO constituent to promote phase separation is rated as MgO > ZnO > CaO > SrO > BaO, which coincides with the order of the cationic field.

The tendency towards phase separation of the SiO_2–B_2O_3–RO–ZrO_2 system without the addition of

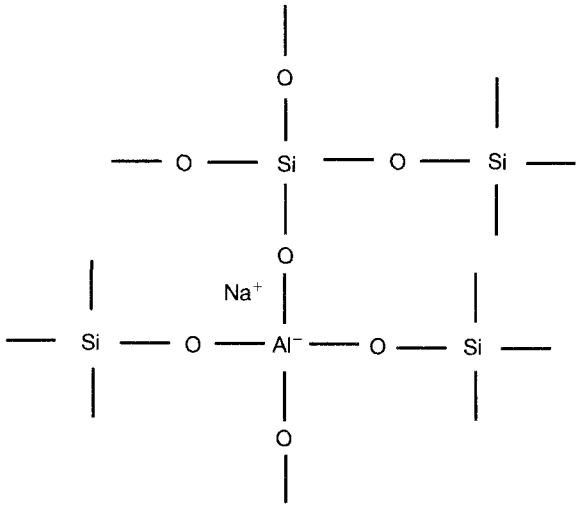

Figure 15 Schematic representation of $[AlO_4]$–$[SiO_4]$ glass network.

Al_2O_3 and Na_2O is so large that it cannot be controlled, as already described. These additives make a strong combination to reduce the phase separation to a moderate level. The effect is explained as follows. Al^{3+} forms $[AlO_4]$ tetrahedra and constructs a glass network with $[SiO_4]$ tetrahedra when their charges are compensated by the Na^+ ions, as pictured in Fig. 15. Thus the introduction of Al_2O_3 with Na_2O imparts an ionic character to the network and increases the compatibility of the network with the boron–oxygen network which also has an ionic character. Thus the tendency of the glass towards phase separation is reduced to a moderate level [12]. The fact that the mole ratio of Na/Al in the SiO_2-rich phase remains approximately 1, despite the composition change with heat-treatment temperature, as shown in Table III, supports this argument. Consequently, the phase separation of this system can be controlled by the addition of these components.

4.2. Composition of porous glass

G–O mother glass without the RO constituent also undergoes phase separation and can be leached with acid. The glass structure is disintegrated during the following alkali treatment, however. The very low alkali resistance of the porous glass indicates that the ZrO_2 content is low. Thus it is concluded that the addition of RO constituent to mother glass is effective in distributing ZrO_2 in the silica-rich phase and consequently in the skeleton of the porous glass. RO brings the other components such as B_2O_3 and Al_2O_3 into the silica-rich phase as well. In addition, the contents of ZrO_2 and Al_2O_3 of the silica-rich phase increase with heat-treatment temperature, though the CaO content remains constant as shown in Table III. The distribution of the glass components between the silica-rich and borate-rich phases is determined by the topology of the miscibility gap and the tie lines. It appears difficult to elucidate these subjects, however, because the composition of the mother glass system is complicated. The interaction of two immiscible regions originating from the SiO_2–B_2O_3–RO system and the SiO_2–B_2O_3–Na_2O system is inferred to entangle the phase separation behaviour. Therefore, the elucidation of the subject requires further investigation.

4.3. Growth of phase-separated structure

Many investigators, using nuclear magnetic resonance- [13], ultraviolet–visible- [14], and Raman spectroscopies [15], and the study of the chemical durability of Pyrex-type glasses [16], have indicated that many sodium borosilicate glasses are phase separated on a nanometre scale even before the heat treatment for phase separation. The following phase-separation process corresponds to the growth of the phase-separated structure under interfacial energy as the driving force. Assuming that the process at the interface is rate controlling, Haller [17] has proposed the following equation for the change in surface area accompanied by the growth of a phase-separated structure

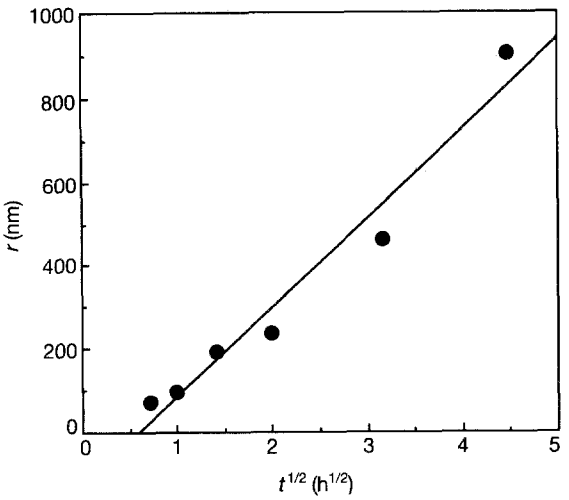

Figure 16 Relationship between heat-treatment time and pore radius. P–Ca glass, heat treated at 750 °C.

$$1/(A^2t) = K\exp[-E/(RT)] \quad (1)$$

where A, T, t, K, E and R are the specific surface area of porous glass, the absolute temperature, the time of heat treatment for phase separation, a constant dependent on glass composition, the activation energy of diffusion, and the gas constant, respectively. Assuming that the shape of the pore is cylindrical, the relationship between pore radius, r, pore volume v, and the specific surface area of a porous glass can be represented as

$$A = (2v)/r \quad (2)$$

Substituting Equation 2, Equation 1 gives

$$r^2 = 4Kv^2t\exp[-E/(RT)] \quad (3)$$

Consequently, the following equation is obtained.

$$r = K't^{1/2} \quad (4a)$$

$$K' = 4Kv\exp[-E/(RT)] \quad (4b)$$

Fig. 16 shows the relation between r and $t^{1/2}$. As shown, r is linearly related to $t^{1/2}$. This result indicates that the above assumption holds in the present system.

5. Conclusion

The alkali-resistant porous glass was prepared from the SiO_2–B_2O_3–RO system containing Al_2O_3, Na_2O and ZrO_2. The porous glass skeleton contained 2–3 mass % ZrO_2 and the alkali resistance was greatly improved over that of ordinary Vycor-type porous glass. Although the effects of RO on the ZrO_2 content in the porous glass skeleton are not yet clarified, they are considered to be controlling components. In particular, CaO and ZnO are practically important in the production of porous glasses. Because of high alkali resistance, the elimination of the gelated SiO_2 and ZrO_2 was promoted and, as a result, a very sharp pore-size distribution was attained. In addition, the limit of the available pore size of the porous glass was widely expanded.

References

1. H. TANAKA, T. YAZAWA, K. EGUCHI, H. NAGASAWA, N. MATSUDA and T. EINISHI, *J. Non-Cryst. Solids* **65** (1984) 301.
2. H. TANAKA, T. YAZAWA, K. EGUCHI and T. YAMAGURO, *Yogyo-Kyokai-Shi* **92** (1984) 492.
3. R. K. ILER, "The Chemistry of Silica" (Wiley, New York, 1976) p. 31.
4. A. J. MAJUMDAR and J. F. RYDER, *Glass Technol.* **9** (1968) 78.
5. K. EGUCHI, H. TANAKA, T. YAZAWA and T. YAMAGURO, in "Proceedings of the 86 Annual Meeting of the Ceramic Society of Japan", Tokyo, May 1986, p. 493.
6. T. YAZAWA, H. TANAKA, K. EGUCHI, S. YOKOYAMA and T. ARAI, *J. Mater. Sci. Lett.* **12** (1993) 263.
7. J. VOLDAN, in "Proceedings of the 11th International Congress on Glass", Prague Vol. 2 (1977) p. 57.
8. P. TAYLOR and D. G. OWEN, *J. Non-Cryst. Solids* **42** (1980) 143.
9. R. W. CRANSTON and F. A. INKLEY, *Adv. Catal.* **9** (1957) 143.
10. R. KURODA, "New Collective Volumes of Experimental Chemistry 9(1)" (Maruzen, Tokyo, 1981) pp. 77, 116.
11. T. YAZAWA, H. TANAKA and K. EGUCHI, *J. Mater. Sci. Lett.*, to be published.
12. Y. MORIYA, *Yogyo-Kyokai-Shi* **78** (1970) 24.
13. M. IMAOKA, H. HASEGAWA, Y. HAMAGUCHI and Y. KUROTAKI, *ibid.* **79** (1971) 164.
14. H. TOYUKI, *ibid.* **86** (1978) 36.
15. W. B. WHITE, *J. Non-Cryst. Solids* **49** (1982) 321.
16. R. H. DOREMUS, "Glass Science" (Wiley, New York, 1973) p. 245.
17. W. HALLER, *J. Chem. Phys.* **42** (1965) 686.

Received 4 May 1993
and accepted 10 January 1994